The origin of the complex character of the Ohmic impedance

C. Blanc[a], M.E. Orazem[b,*], N. Pébère[a], B. Tribollet[c], V. Vivier[c], S. Wu[b]

[a] Université de Toulouse, CIRIMAT, UPS/INPT/CNRS, ENSIACET 4, allée Emile Monso, BP 44362, 31432 Toulouse cedex 4, France
[b] Department of Chemical Engineering, University of Florida, Gainesville, FL 32611, USA
[c] Laboratoire Interfaces et Systèmes Electrochimiques, UPR 15 du CNRS, Université Pierre et Marie Curie, 75252 Paris cedex 05, France

A B S T R A C T

The local and global Ohmic response for an electrode exhibiting geometry-induced potential and/or current distributions has recently been shown to be represented by a frequency-dependent complex impedance. A physical explanation for this result is provided in terms of the radial contribution to local current density and the decrease in current density along the current lines. Experiments performed with Cu/Al and Mg/Al galvanic couples show that, in regions where a radial current density does not exist, the local Ohmic impedance is independent of position; whereas, in regions where the radial current density cannot be neglected, the local Ohmic impedance is a function of position. Simulations performed on recessed electrodes show that, even in the absence of a radial current, an axial variation of current density gives rise to a complex Ohmic impedance. The complex character of the Ohmic impedance shows that an equivalent circuit, using the usual two-terminal resistor to represent the Ohmic contribution of the electrolyte, provides an inadequate representation of an electrode with geometry-induced current and potential distributions.

Keywords:
Local electrochemical impedance
Galvanic coupling
Current and potential distributions
Mathematical model

1. Introduction

The electrochemical impedance is generally separated into two parts, one part corresponding to the interface which includes the double layer capacitance, the Faradaic impedance and, if necessary, an impedance corresponding to a deposit or coating; and a second part corresponding to the Ohmic drop in the electrolyte. This Ohmic contribution is usually represented by a pure resistor. In many experiments, this contribution is minimized, for instance by diminishing the distance between the reference electrode and the working electrode, but it cannot be omitted. The Ohmic resistance depends on the electrolyte conductivity and on the cell geometry (i.e. electrode size and positions). For instance, Newman [1], by solving the problem of primary current distribution for a disk electrode of radius r_0 embedded in an infinite insulating plane and with a hemispherical counterelectrode at infinity, gave the corresponding electrolyte resistance as

$$R_e = \frac{1}{4\kappa r_0} \tag{1}$$

where κ is the conductivity of the solution. This resistance is represented in the equivalent electrical circuit by a resistor in the form of a two-terminal element.

* Corresponding author at: Department of Chemical Engineering, University of Florida, PO Box 116005, Gainesville, FL 32611, USA.
E-mail address: meo@che.ufl.edu (M.E. Orazem).

The impedance response of electrochemical systems often reflects a distributed reactivity. The local variation of impedance was considered by Brug et al. [2] to investigate the CPE behavior of a blocking electrode. In the schematic representation of the interface (Fig. 1), the local electrolyte resistance appears as having a constant value along the radial coordinate, and the interfacial capacitance $C_0(r)$ is distributed along the electrode surface.

In the recent development of local electrochemical impedance analysis [3–5], concepts of local impedance were revisited taking advantage of the possibility of measuring the local ac-current density in the close vicinity of the interface [6–8]. Huang et al. [3–5] defined the local interfacial impedance z_0 to be

$$z_0 = \frac{\tilde{V} - \tilde{\Phi}_0}{\tilde{i}} \tag{2}$$

the local Ohmic impedance z_e to be

$$z_e = \frac{\tilde{\Phi}_0 - \tilde{\Phi}_\infty}{\tilde{i}} \tag{3}$$

and local impedance z, which is the sum of Eqs. (2) and (3), to be

$$z = z_0 + z_e = \frac{\tilde{V} - \tilde{\Phi}_\infty}{\tilde{i}} \tag{4}$$

In these definitions, $\tilde{V} - \tilde{\Phi}_0$ represents the ac-potential difference between the electrode surface and a point just outside the double-layer, $\tilde{\Phi}_0 - \tilde{\Phi}_\infty$ represents the ac-potential difference between a point just outside the double layer and the refer-

doi:10.1016/j.electacta.2010.04.036

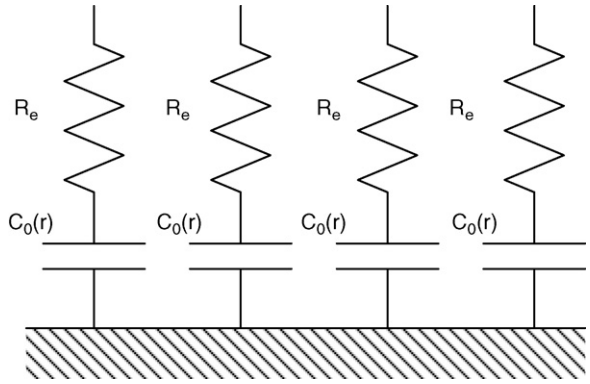

Fig. 1. Representation of an idealized polarized electrode according to Brug et al. [2]. R_e is independent of the radial position; whereas, C_0 depends on the radial position. The Ohmic resistance is represented as a two-terminal element.

ence electrode in the bulk solution, and $\tilde{V} - \tilde{\Phi}_\infty$ represents the ac-potential difference between the electrode surface and the reference electrode in the bulk solution. The quantity $\tilde{V} - \tilde{\Phi}_\infty$ is the applied ac-perturbation to the electrochemical system.

The corresponding definitions are illustrated in Fig. 2 in terms of local electrical equivalent circuits. The arrows show the usual understanding of the flow of the time-dependent current density through the Ohmic impedance and then splitting into Faradaic (R_t) and capacitive (C_0) components. A cylindrical coordinate system was used in this work such that the axial coordinate is normal to the electrode surface.

For an idealized polarized electrode, R_t is infinite and the only difference between Figs. 1 and 2 is the physical nature of the Ohmic impedance. In Fig. 1, the Ohmic impedance corresponds to a pure resistor (electrolyte resistance) with a real and uniform value along the electrode radius; whereas, in Fig. 2, the Ohmic impedance is a complex quantity that depends on the radial coordinate. Huang et al. [3–5] have shown that, for a disk electrode embedded in an insulating plane, the local Ohmic impedance is a complex number with a non-negligible imaginary part. Such an Ohmic contribution can be experimentally observed on blocking electrode [4] or for more complicated reaction mechanism involving adsorbates [9,10]. As a consequence, the local impedance experimentally measured shows inductive behavior at high frequency [4,11–13].

The complex Ohmic impedance originates in the nature of the current distribution within the electrolyte. For both an ideally

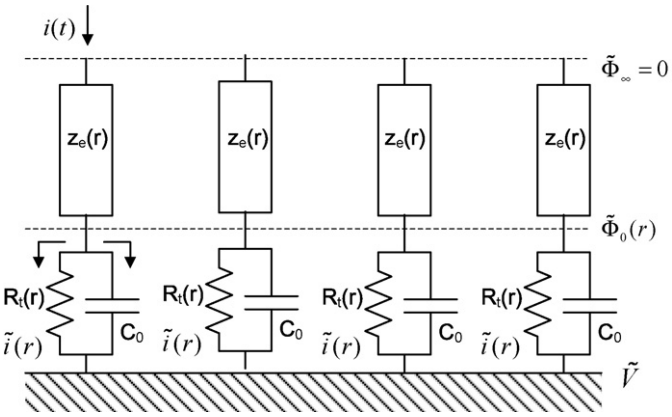

Fig. 2. Schematic representation of an impedance distribution for a disk electrode where z_e represents the local Ohmic impedance, C_0 represents the interfacial capacitance, and R_t represents the charge-transfer resistance. The arrows show the flow of time-dependent current density through the Ohmic impedance and splitting into Faradaic and capacitive components. [5].

polarized electrode (Fig. 1) and a non-ideally polarized electrode (Fig. 2), the potential $\Phi_0(r)$ of a reference probe located at the outer limit of the diffuse double layer depends on its radial position. A nonzero difference of potential exists between two radially separated points equidistant from the electrode surface and just outside the diffuse double layer. Thus, according to Ohm's law, a radial contribution of the current must exist and is defined as

$$i_r = -\kappa \frac{\partial \Phi}{\partial r} \tag{5}$$

However, the electrical representation of the electrochemical cells presented in Figs. 1 and 2 does not account for such a radial current because only normal pathways to the electrode surface are considered.

Newman et al. [14–16] demonstrated, for a disk electrode in an insulating plane, that the potential distribution is nonuniform when the current distribution is uniform, and, conversely, the current distribution is nonuniform under conditions where the potential is uniform. As explained above, a consequence of a nonuniform potential distribution is the existence of a radial current; thus, when the normal current density follows a primary distribution, the radial current does not exist and when the normal current is uniform the radial current has a nonzero value. Moreover, these effects are frequency-dependent since the distributions of potential and current along the disk also depend on frequency.

The objective of the present work is to understand, on a physical basis, the parameters that contribute on local impedance diagrams to the inductive behavior observed at high frequency, and in particular, to investigate the influence of current and potential distributions. In order to explore radial and normal current distributions, three different configurations were studied. First, simple systems consisting in two model couples were investigated: a pure copper/pure aluminum (Cu/Al) couple and a pure magnesium/pure aluminum (Mg/Al) couple. For the two model couples, the galvanic coupling between the two metals increases the radial current. Experimental results were compared with numerical simulations of potential and current distributions on the surface of the model couples at the beginning of immersion. The second case concerned a recessed electrode for which the radial current can be eliminated. In this case, calculations were performed for a blocking electrode. Finally, the origin of the frequency dependence on the Ohmic impedance was shown for a disk electrode with a single-step-Faradaic reaction.

2. Experimental

2.1. Samples

The samples consisted of pure magnesium/pure aluminum and pure copper/pure aluminum couples. A cylinder of pure aluminum (99.999 wt%—Alfa Aesar) was drilled in its center and a cylinder of pure magnesium (99.9 wt%—Alfa Aesar) was introduced by force into the hole. The assembly of the two materials gave a perfectly joined interface, avoiding any crevice corrosion due to surface defects. The cylinder diameters were chosen to obtain an aluminum/magnesium surface area ratio of about 10 (the radii were 1 and 0.32 cm for the aluminum and magnesium bars, respectively). Similarly, a cylinder of pure aluminum was drilled in its center and a cylinder of pure copper (99.9 wt%—Goodfellow) was then introduced by force into the hole. The surface ratio of the two electrodes was also 10. The electrodes were then embedded in an epoxy resin. Before immersion in the electrolyte, the disk electrodes were mechanically polished with SiC papers down to 4000 grade and ultrasonically cleaned with ethanol, then with distilled water. The electrolyte was a 10^{-3} M Na_2SO_4 solution prepared with analytical grade chemicals at room temperature.

2.2. Local electrochemical measurements

The corrosion behavior of the model couples was studied by local electrochemical impedance spectroscopy (LEIS). The measurements were carried out with a Solartron 1275 system. The method used a five-electrode configuration. The disk in an insulating plane represented the working electrode with potential measured with respect to a distant reference electrode. A counter electrode was placed far from the disk electrode. Two sensing electrodes were employed in a small bi-electrode probe used for local current density measurements. Details are provided elsewhere [17–19]. The bi-electrode probe was stepped across a selected area of the sample. The analyzed part had an area of 2.4×2.4 cm and the step size was 500 μm in the *X* and *Y* directions. The local impedance diagrams were recorded over a frequency range of 3 kHz to around 300 mHz with six points per decade. The local impedance measurements were carried out in a low conductivity 10^{-3} M Na_2SO_4 solution (10^{-4} S cm^{-1}) to optimize resolution of the local current measurement. With the experimental set up used, only the normal component of the current could be measured.

2.3. Numerical analysis

All calculations were performed using the finite element package Comsol® for solving Laplace's Equation in a 2D axis-symmetry geometry. The detailed implementation of the equation and boundary conditions was previously described elsewhere [12,20].

3. Results

The experimental and simulation results are presented in this section.

3.1. Galvanic coupling between copper/aluminum and magnesium/aluminum

Pure Cu/Al and pure Mg/Al couples were devised in order to give rise to radial and normal current distributions. These two model couples were initially designed to study corrosion phenomena associated with intermetallics in aluminum alloys in previous investigations [21,22]. In the Cu/Al couple, aluminum is the anode of the system and is in the passive state while copper is polarized cathodically. In the Mg/Al couple, magnesium acted as the anode of the system whereas, both oxygen and water reduced on aluminum, which behaves as a cathode.

3.1.1. Pure copper/pure aluminum

The potential distribution calculated on the electrode surface along the electrode radius is presented in Fig. 3a. The potential distribution is uniform on copper and nonuniform on aluminum. The corresponding current distributions are presented in Fig. 3b and c. In agreement with the Newman's predictions [14–16], the potential distribution on copper is uniform and the normal current distribution is nonuniform. Accordingly, the radial current is uniform. In contrast, the potential distribution on aluminum is nonuniform, the normal current distribution is uniform, and the radial current distribution is nonuniform.

Local impedance spectra measured at different radial positions are presented in Fig. 4. The high-frequency inductive loop is attributed to the local Ohmic impedance [3–5]. It appears clearly that on copper, where the potential distribution is uniform and the radial current density is equal to zero (Fig. 3), the local Ohmic impedance is not distributed even though a clear inductive loop is measured. In contrast, on aluminum, where the potential distribution is nonuniform, the radial current is not equal to zero, and the local Ohmic impedance is distributed along the radius.

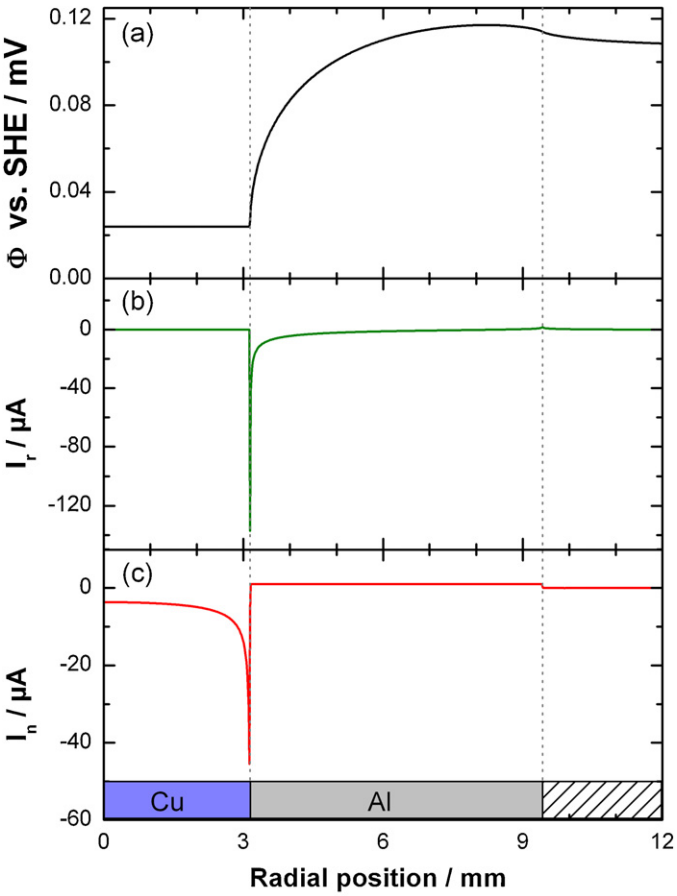

Fig. 3. (a) Potential distribution on the surface of the Cu/Al model couple deduced from theoretical calculations for an electrolyte conductivity of 5×10^{-5} S/cm; (b) radial current distribution and (c) normal current distribution [21].

On both copper and aluminum parts of the electrode, the local Ohmic impedance is represented by a complex quantity. The local Ohmic impedance is independent of the radial position when the radial current is equal to zero, and it depends strongly on the radial position when the radial current is not equal to zero. It should be noticed that such a behavior has already been observed but not interpreted in the pioneering work of Isaacs on local impedance [6] for the Mo/Al system.

3.1.2. Pure magnesium/pure aluminum

The polarization of the Al electrode changes in the Mg/Al system. For the Mg/Al couple, Al acts as a cathode and Mg is the anode [22]. The potential distribution on magnesium is uniform, the normal current distribution is nonuniform, and the radial current density near the interface has a zero value. On aluminum, in contrast, the potential distribution is nonuniform, the normal current distribution is uniform, and the radial current density near the interface is not equal to zero [22].

Local impedance measurements were performed on both electrodes with the radial position of the bi-electrode as a parameter. Over the Mg electrode (Fig. 5) the high-frequency inductive loops are attributed to the local Ohmic impedance and are clearly independent of the radial position. In this case also, when the radial current has a zero value or when there is no potential distribution, the local Ohmic impedance is independent of the radial position.

Conversely, the local impedance diagrams measured on the aluminum electrode for different radial positions (Fig. 6) show a high-frequency inductive loop that depends on the radial position. Again, when the potential is distributed, the radial current

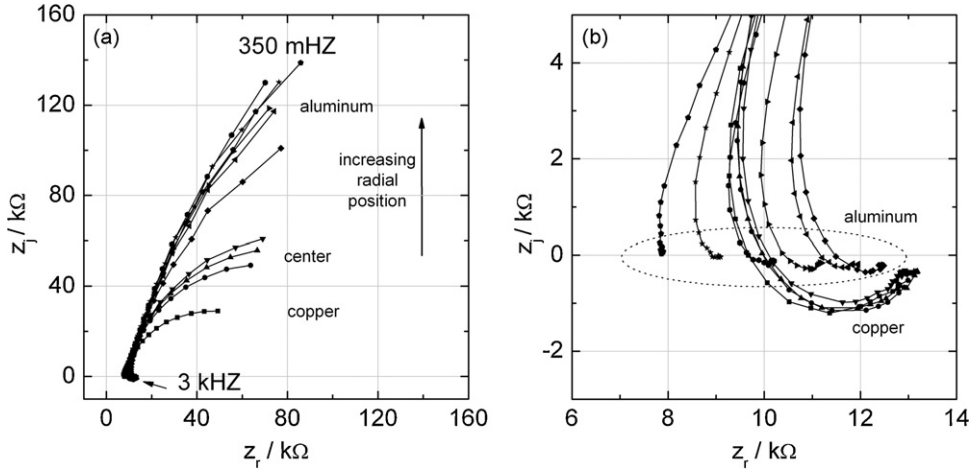

Fig. 4. Local electrochemical impedance spectra measured along the Cu/Al electrode radius: (a) frequency range from 3 kHz to 350 mHz; and (b) an expanded view of the high frequency part.

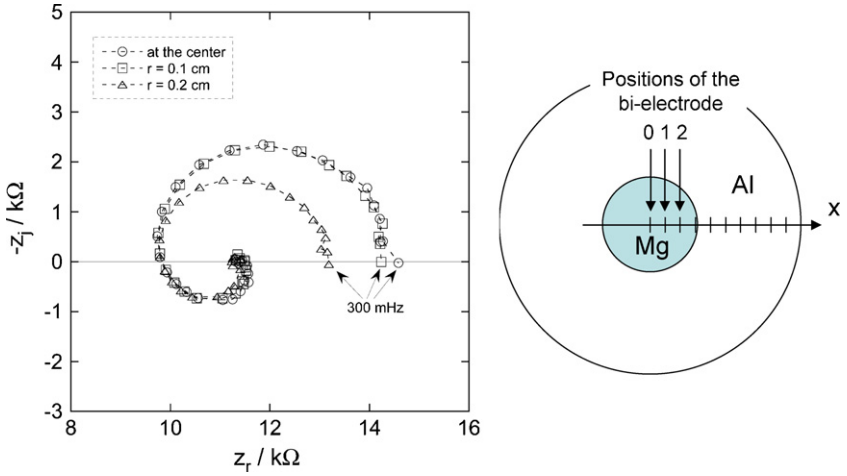

Fig. 5. Local impedance spectra obtained on the magnesium electrode with the radial position as a parameter.

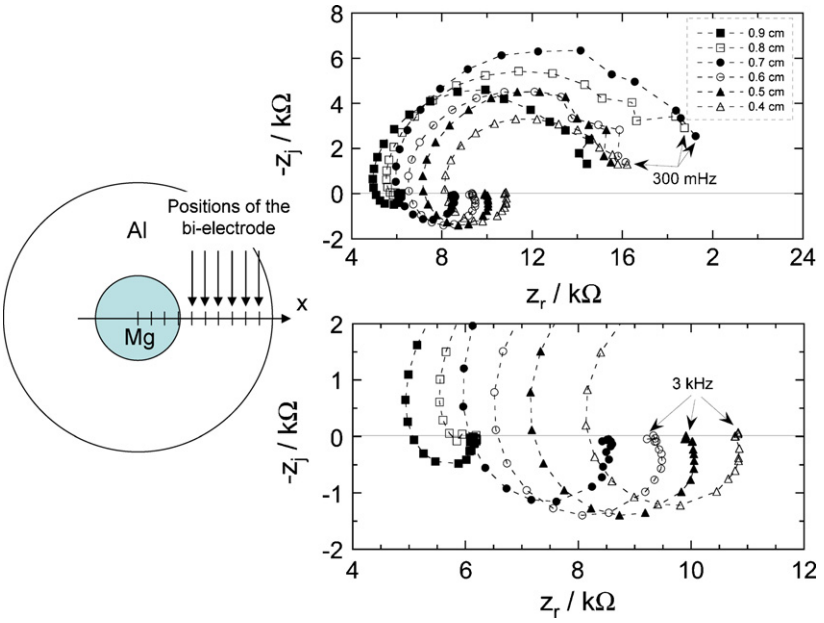

Fig. 6. Local impedance spectra obtained on the aluminum electrode with the radial position as a parameter.

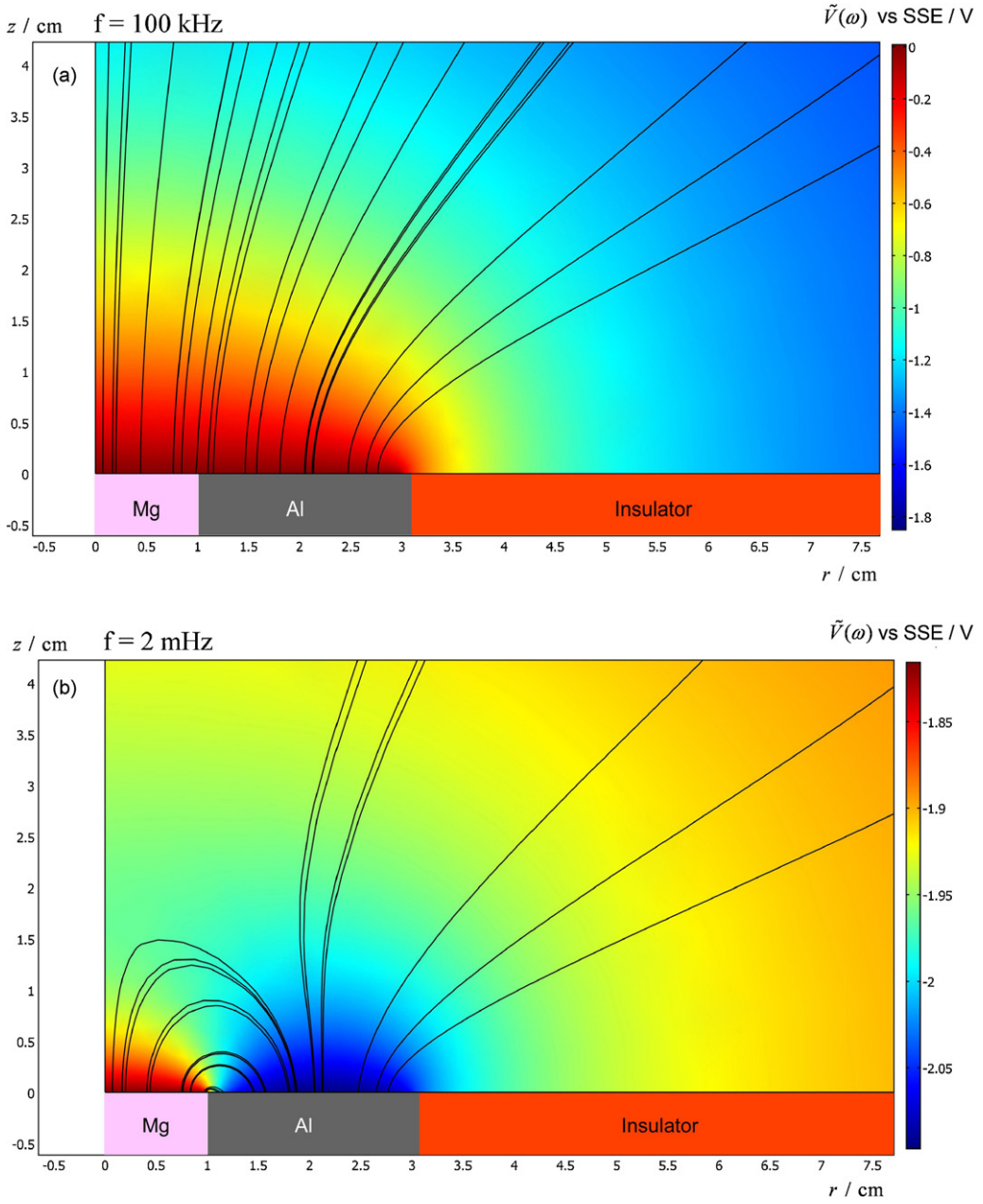

Fig. 7. Calculated current and potential (vs. SSE/V) distributions for a Mg/Al couple obtained at two different frequencies: (a) 100 kHz; and (b) 2 mHz.

is nonzero and the local Ohmic impedance varies with the radial position.

3.1.3. LEIS numerical simulations for galvanic coupling

Numerical calculations were undertaken for the Mg/Al couple to verify that these effects only reflect the geometry of the system and the galvanic coupling. Simulations were performed under the assumptions that:

- the potential is governed by the Laplace equation,
- the net dc-current over the electrode surface is equal to zero [21,22],
- a large counterelectrode was located far from the working electrode in the electrochemical cell, and
- the reference electrode and counterelectrode are at the same potential.

By solving Laplace's equation for the sinusoidal steady-state condition, the local impedance could be calculated for different radial positions. The results of this simulation are given in Figs. 7 and 8.

The calculated distributions of current and potential are presented in Fig. 7 for high and low frequencies. At 100 kHz, the potential distribution corresponds to the primary potential distribution and is consistent with the previous work of Newman [1]. This primary current distribution depends on the diameter of the disk electrode formed by the couple Mg/Al and the use of a hemispherical counterelectrode located at infinity allows the electrolyte resistance to satisfy Eq. (1). In contrast, for a frequency of 2 mHz (Fig. 7b), the current and potential distributions are similar to the distributions obtained for the dc case and have been discussed in Ref. [22].

The calculated local impedance spectra (Fig. 8) provide qualitative agreement with the experimental spectra. On the magnesium,

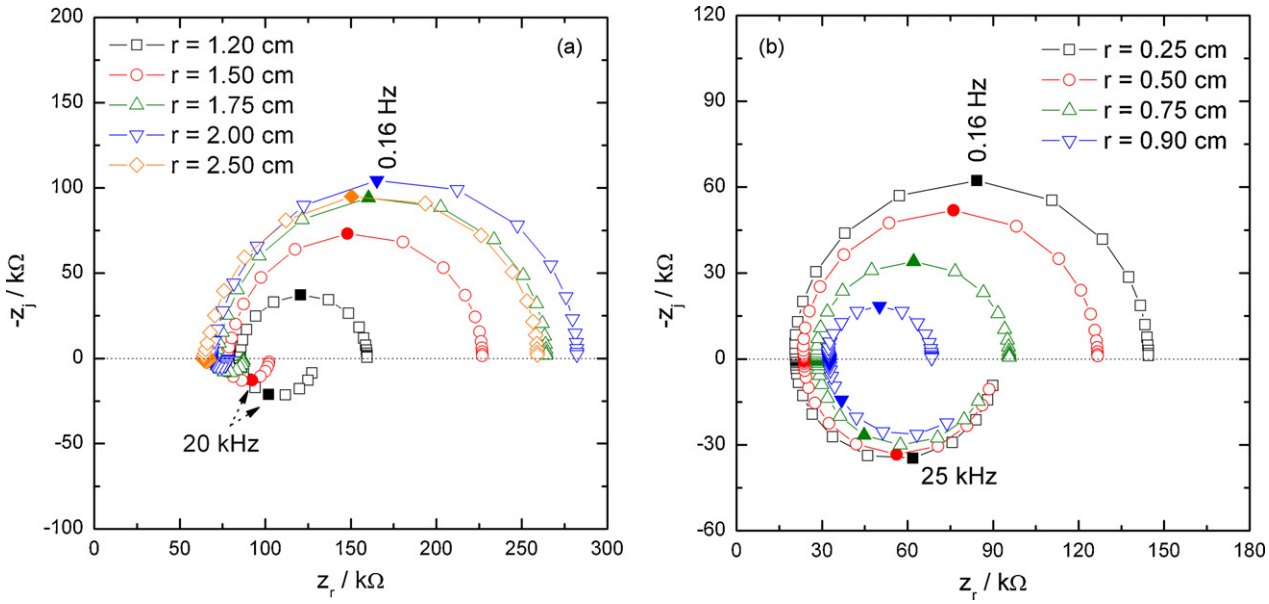

Fig. 8. Calculated local impedance spectra with radial position as a parameter for an electrode with galvanic coupling between magnesium at the center and aluminum: (a) aluminum and (b) magnesium.

the high-frequency inductive loop is independent of the radial position; whereas, on the aluminum, the high-frequency inductive loop depends on the radial position. These calculations were in fairly good qualitative agreement with experimental results. The discrepancies observed between experiment and numerical calculations were attributed to the fact that the system used for performing local impedance measurements could not provide the precise conditions assumed for calculations.

The above work demonstrates that the complex character of the Ohmic impedance can be attributed in part to the presence of a radial current density in the electrolyte outside the diffuse double layer. However, local Ohmic impedance is observed as well along the centerline of the electrode where, by axial symmetry, the radial current density is identically equal to zero. Thus, while a radial current distribution must influence the Ohmic impedance away from the centerline, an additional contribution must be attributed to the decrease, associated with the disk geometry, of the current density with axial position, as discussed by Frateur et al. [12]. The role of changes in current density with axial position was explored by simulations performed for recessed electrodes.

3.2. Recessed electrode

The objective of this part of the work was to explore by numerical simulation the influence of the recessed geometry of a disk electrode on the local and global Ohmic impedance for an ideally polarized electrode. The geometry and the position of the reference (or counter) electrode were shown to play a significant role on the numerical result of the calculated impedance. Thus, a spherical geometry and a distance between the working electrode and the counterelectrode 2000 times larger than the disk electrode radius were used to perform numerical calculation in order to reach an error range smaller than 0.2%. The corresponding experimental electrochemical cell was described in [12].

Local Ohmic impedance spectra corresponding to two radial positions are presented in Fig. 9 in terms of dimensionless frequency

$$K = \frac{\omega C_0 r_0}{\kappa} \tag{6}$$

with the dimensionless recessed electrode depth $P = p/r_0$ as a parameter where p is the depth of the recessed cavity. The nominal Ohmic resistance associated with the cavity is subtracted in Fig. 9 from the real part of the Ohmic impedance, which serves to emphasize the contribution associated with the electrolyte above the cavity. When the recessed electrode depth increases, the loop corresponding to the local Ohmic impedance decreases in size and tends towards a real number. For a sufficient depth, the geometry-induced current and potential distributions are negligible, and the local Ohmic impedance approaches the same value for the two radial positions $r/r_0 = 0$ and $r/r_0 = 0.6$.

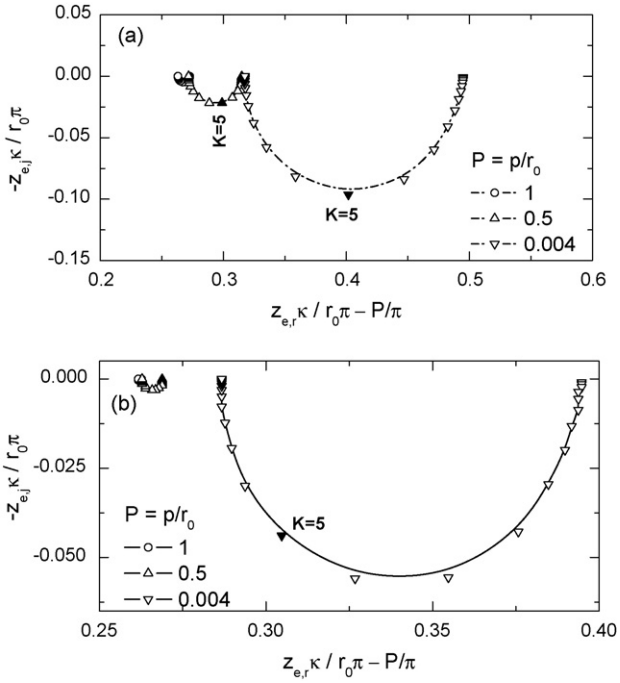

Fig. 9. Calculated values for local Ohmic impedance at the electrode surface with the recessed electrode depth as a parameter: (a) $r/r_0 = 0$ and (b) $r/r_0 = 0.6$. Adapted from Ref. [12].

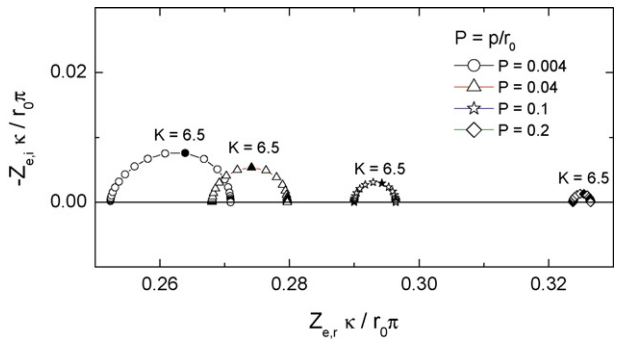

Fig. 10. Calculated global Ohmic impedance with dimensionless recessed electrode depth as a parameter.

The corresponding global Ohmic impedance is given in Fig. 10 with the recessed electrode depth as a parameter. When P tends towards zero, the situation is identical to the case study presented by Newman for an ideally polarized electrode [23].

Recently, experimental local electrochemical measurements performed with bi-electrode and with microcapillary technique showed a divergence due to the Ohmic impedance [13]. For the bi-electrode, the Ohmic impedance in the complex plane had an inductive loop and, for the microcapillary, which is similar to a recessed electrode, the Ohmic impedance is real. These results are in perfect agreement with those obtained in the present study.

3.3. *Influence of frequency for a Faradaic reaction*

The preceding work was used to demonstrate the role that axial and radial current density distributions have on the appearance of a complex character in the Ohmic response of the electrolyte. Huang et al. [3–5] have shown that the contribution of the imaginary part of the Ohmic impedance is dependent on frequency. The Ohmic impedance approaches a real number corresponding to the primary resistance at high frequency and a different real number at low frequency. The origin of the frequency dependence of the imaginary part of the Ohmic impedance can be inferred through examination of the local oscillating potential, shown in Fig. 11 with frequency as a parameter. The simulations were performed for a disk electrode subject to a single-step Faradaic reaction with $J = 4R_e/\pi R_t = 1$ [5]. The local Ohmic impedance, given in Eq. (3), can be expressed as

$$z_e = \frac{\tilde{\Phi}_0}{\tilde{i}} \tag{7}$$

where the potential is referenced to the fixed value $\tilde{\Phi}_\infty$. The distribution of local Ohmic impedance is given in Fig. 12.

Due to the numerical limitations described by Newman [23], the simulations were not reliable for dimensionless frequencies K greater than 100. Nevertheless, the results can be used to show that, at high frequency, e.g., $K > 100$, the real and imaginary parts of the complex potential $\tilde{\Phi}_0$ tend to be uniform and the imaginary part of the potential becomes very small. This corresponds physically to the condition under which the charging current dominates as compared to the current associated with the Faradaic reaction. At low frequencies, the real part of the potential is not uniform, but the imaginary part of the potential tends toward zero. This corresponds physically to the condition under which the current associated with the Faradaic reaction dominates. Both the corresponding low-frequency and high-frequency local Ohmic impedances shown in Fig. 12 are not uniform, but the imaginary parts tend to zero (see also Fig. 11 in Ref. [5]). The imaginary part of the local Ohmic impedance plays a significant role between $K = 1$ and $K = 10$ where, as seen in Fig. 11b, $\tilde{\Phi}_{0,j}$ has a maximum value. The value $K = 1$ corresponds to frequency $\omega = (R_e C_0)^{-1}$, as discussed by Huang et al. [5].

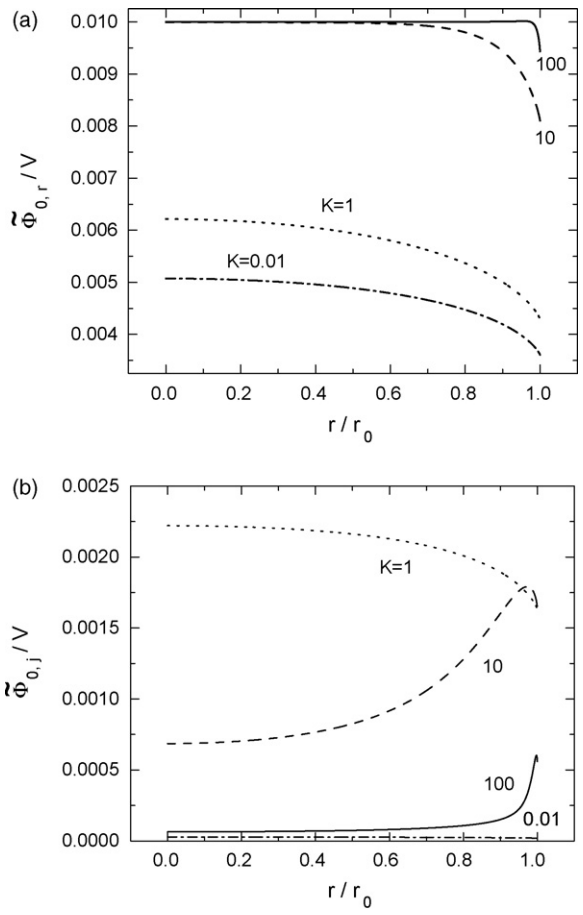

Fig. 11. Calculated distribution of the oscillating interfacial potential for a disk electrode with a single-step Faradaic reaction with $J = 1$: (a) real part and (b) imaginary part.

4. Discussion

The global overall impedance for ideally polarized disk electrodes exhibiting geometry-induced current and potential distributions has been calculated and shown to exhibit time-constant dispersion. The effect is seen for dimensionless frequency $K = \omega C_0 r_0/\kappa > 1$, which can be within the experimentally accessible range [2]. This result, which applies as well to disk electrodes under linear kinetics, was first reported by Newman in 1970 [23].

The origin of the time-constant dispersion is represented in the present work in the form of a complex Ohmic impedance. To see that this approach is in agreement with Newman's results, consider a blocking interface with a frequency-independent capacitance C_0 and an interfacial impedance $Z_0 = 1/j\omega C_0$. This interfacial impedance is independent of the electrode geometry. The measured overall impedance, which includes the Ohmic contribution, is $Z = Z_e + 1/j\omega C_0$, where the capacitance C_0 is independent of frequency and Z_e is termed the Ohmic impedance. Newman, in contrast, represented the overall impedance as the sum of a frequency-dependent resistance R_{eff} in series with a frequency-dependent capacitance C_{eff}. The two descriptions of the same phenomena give

$$Z_e + 1/j\omega C_0 = R_{\text{eff}} + 1/j\omega C_{\text{eff}} \tag{8}$$

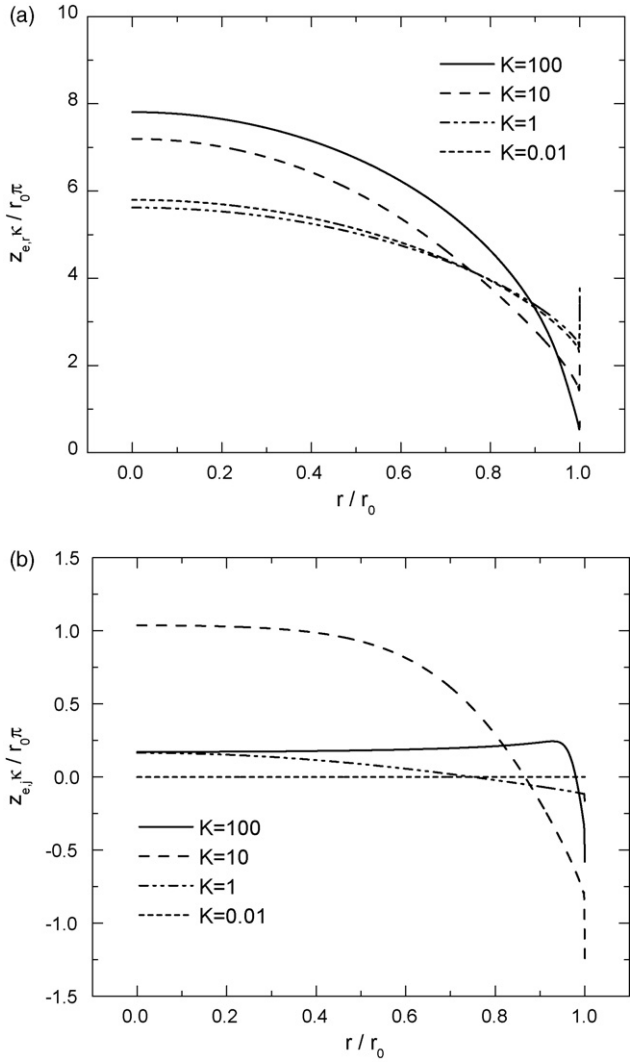

Fig. 12. Calculated distribution of the local Ohmic impedance for a disk electrode with a single-step Faradaic reaction with $J = 1$: (a) real part and (b) imaginary part.

which yields

$$Z_e = R_{\text{eff}} - \frac{j}{\omega}\left(\frac{C_0 - C_{\text{eff}}}{C_0 C_{\text{eff}}}\right) \tag{9}$$

The fact that Z_e is frequency-dependent is in perfect agreement with Newman's result [23]. When the frequency tends towards infinity, the current distribution corresponds to the primary current distribution and $\lim_{\omega\to\infty} Z_e = 1/4\kappa r_0$, in agreement with Newman's formula.

It is important to note that the complex character of the Ohmic impedance is not only a property of the electrolyte but is instead a property of the electrode geometry, of the interfacial impedance, and of the electrolyte with conductivity κ. The interfacial impedance can correspond to an ideally polarized electrode but also to Faradaic reactions with or without adsorbed intermediates. A complex Ohmic impedance is not seen for recessed electrodes for which both the current density and interfacial potential are uniform.

For the different cases considered in this work, the local Ohmic response also takes the form of a complex frequency-dependent impedance. The local Ohmic impedance varies with position when a radial current is present due to the presence of a potential distribution. In absence of potential distribution and in presence of a normal current distribution, the local Ohmic impedance can have a complex value, but, in this case, the value is independent of the radial position.

The observation that the local Ohmic impedance has a complex value, even on the electrode axis, where, for reasons of symmetry the radial current density is equal to zero, shows that the Ohmic impedance cannot be explained solely by the fact that the radial current is not taken into account in the equivalent circuit representation. The explanation can be extended to account for the observed phenomenon. In the usual interpretation of a two-terminal element, as was used in Figs. 1 and 2, the current which enters the element must be the same that the current which leaves the element. An explanation for the observed complex Ohmic impedance at the centerline can be found by recognizing that, due to the disk geometry, the current density at the entrance of the two-terminal element is different than the current density which leaves the element. Along a vertical line, the current density decreases with the distance from the electrode. For global impedance, one side of the two-terminal element corresponds to the electrode area and the other side to the surface of the counterelectrode, which is much larger. Due to the frequency dependence of the current distribution on the electrode surface, the variation of the current density along the normal distance to the electrode depends on frequency, which explains why this quantity is represented by a complex value.

While the presence of geometry-induced current and potential distributions can be used to indicate the presence of an Ohmic impedance rather than an Ohmic resistance, exploration of the dependence of the imaginary part of the Ohmic impedance on frequency requires consideration of the oscillating components of potential and current. The relationship between complex oscillating potential and current density is somewhat complicated, but numerical simulations show that the Ohmic impedance approaches a real number at high frequencies and at low frequencies. As discussed by Huang et al., the complex character is seen at an intermediate frequency associated with the R_eC_0 time constant [5].

5. Conclusions

The appearance of the complex Ohmic impedance is attributed to the nonuniform current and potential distributions induced by electrode geometry. For the disk embedded in an insulating plane, the radial current density is a function of radial position and has an associated decrease in current density with axial position. In this case, the Ohmic impedance must be represented by a complex number. For the recessed disk electrode geometry, there is no radial current and the current density is independent of axial position. In this case, the Ohmic impedance can be represented by a real number. The complex character of the Ohmic impedance is therefore not only a property of electrolyte conductivity, but also a property of electrode geometry and interfacial impedance.

The experiments performed with galvanic couples eliminated, over a portion of the disk surface, the radial current density, but did not eliminate the axial variation of current density. In this case, the Ohmic impedance was still represented by a complex number, but this value was independent of radial position. In cases where the radial current density was not eliminated, the complex local Ohmic impedance was a function of radial position. This work shows that the local variation of axial and radial current density causes the Ohmic contribution to be represented by a complex number.

The local Ohmic impedance represents the impedance between a point just outside the diffuse double-layer and a hemispherical counter electrode at infinity. This impedance takes into account the possible existence of a radial current and the variation of the current density along the direction normal to the electrode. The global Ohmic impedance represents the mean value of the local

Ohmic impedance over the electrode and it is represented by a complex quantity for the same reasons. The complex character of the Ohmic impedance seems counter-intuitive when the disk electrode is represented by an equivalent circuit using the usual two-terminal resistor to represent the Ohmic contribution of the electrolyte. While representation of the impedance by an equivalent electric circuit can be convenient, this simplified representation may also cause misunderstanding.

References

[1] J.S. Newman, Electrochemical Systems, 2nd edition, Prentice Hall, Englewood Cliffs, NJ, 1991.
[2] G.J. Brug, A.L.G. van den Eeden, M. Sluyters-Rehbach, J.H. Sluyters, J. Electoanal. Chem., Interfacial Electrochem. 176 (1984) 275.
[3] V.M.-W. Huang, V. Vivier, M.E. Orazem, N. Pébère, B. Tribollet, J. Electrochem. Soc. 154 (2007) C81.
[4] V.M.-W. Huang, V. Vivier, I. Frateur, M.E. Orazem, B. Tribollet, J. Electrochem. Soc. 154 (2007) C89.
[5] V.M.-W. Huang, V. Vivier, M.E. Orazem, N. Pébère, B. Tribollet, J. Electrochem. Soc. 154 (2007) C99.
[6] R.S. Lillard, P.J. Moran, H.S. Isaacs, J. Electrochem. Soc. 139 (1992) 1007.
[7] F. Zou, D. Thierry, H.S. Isaacs, J. Electrochem. Soc. 144 (1997) 1957.
[8] E. Bayet, F. Huet, M. Keddam, K. Ogle, H. Takenouti, Electrochim. Acta 44 (1999) 4117.
[9] S. Wu, M.E. Orazem, B. Tribollet, V. Vivier, J. Electrochem. Soc. 156 (2009) C28.
[10] S. Wu, M.E. Orazem, B. Tribollet, V. Vivier, J. Electrochem. Soc. 156 (2009) C214.
[11] P. de Lima-Neto, J.P. Farias, L.F.G. Herculano, H.C. de Miranda, W.S. Araujo, J.-B. Jorcin, N. Pébère, Corros. Sci. 50 (2008) 1149.
[12] I. Frateur, V.M.-W. Huang, M.E. Orazem, N. Pébère, B. Tribollet, V. Vivier, Electrochim. Acta 53 (2008) 7386.
[13] J.-B. Jorcin, H. Krawiec, N. Pébère, V. Vignal, Electrochim. Acta 54 (2009) 5775.
[14] J. Newman, J. Electrochem. Soc. 113 (1966) 1235.
[15] J. Newman, J. Electrochem. Soc. 113 (1966) 501.
[16] W.H. Smyrl, J. Newman, J. Electrochem. Soc. 119 (1972) 208.
[17] G. Baril, C. Blanc, M. Keddam, N. Pébère, J. Electrochem. Soc. 150 (2003) B488.
[18] J.-B. Jorcin, E. Aragon, C. Merlatti, N. Pébère, Corros. Sci. 48 (2006) 1779.
[19] J.-B. Jorcin, M.E. Orazem, N. Pébère, B. Tribollet, Electrochim. Acta 51 (2006) 1473.
[20] I. Frateur, V.M.-W. Huang, M. Orazem, V. Vivier, B. Tribollet, J. Electrochem. Soc. 154 (2007) C719.
[21] J.-B. Jorcin, C. Blanc, N. Pébère, B. Tribollet, V. Vivier, J. Electrochem. Soc. 155 (2008) C46.
[22] L. Lacroix, C. Blanc, N. Pébère, B. Tribollet, V. Vivier, J. Electrochem. Soc. 156 (2009) C259.
[23] J.S. Newman, J. Electrochem. Soc. 117 (1970) 198.